Heat Transfer Enhancement with Nanofluids for Automotive Cooling

Adnan M. Hussein, K. Kadirgama, K.V. Sharma, D. Ramasamy and R.A. Bakar

Abstract The increasing demand of nanofluids for the industrial applications has led to focus on it from many researchers in the last decade. This thesis includes both experimental study and numerical study to improve heat transfer with slightly pressure drop in the automotive cooling system. The friction factor and heat transfer enhancement using different types of nanofluids are studied. The TiO_2 and SiO_2 nanopowders suspended to four different base fluids (pure water, EG, 10 % EG + 90 %W, and 20 %EG + 80 %W) are prepared experimentally. The thermophysical properties of both nanofluids and base fluids are measured and validated with the standard and the experimental data available. The test section is setup including car radiator and the effects under the operating conditions on the heat transfer enhancement analyzed under laminar flow condition. The volume flowrate, inlet temperature, and nanofluid volume concentrations are in the range of (1-5LPM) for pure water and (3-12LPM) for other base fluids, (60–80 °C) and (1–4 %), respectively. On the other side, the CFD analysis for the nanofluid flow inside the flat tube of a car radiator under laminar flow is carried out. A simulation study is conducted by using the finite volume technical to solve the continuity, momentum, and energy equations. The processes of the geometry meshing of problem and describing the boundary conditions are performed in the GAMBIT then achieving of FLUENT software to find the friction factor and heat transfer coefficient. The experimental results show the friction factor decreases with the increase of the volume flowrate and increases with the nanofluid volume fraction but slightly decreases with the increase of the inlet temperature. Furthermore, the simulation results show good agreement with the experimental data with deviation, not more than 4 %. The experimental results show that the heat transfer coefficient increases with the increase in the volume flowrate, the nanofluid volume fraction,

K.V. Sharma
Department of Mechanical Engineering, Universiti Teknologi PETRONAS, 32610 Bandar Seri Iskandar, Perak Darul Ridzuan, Malaysia
e-mail: sharma.korada@petronas.com.my

A.M. Hussein · K. Kadirgama (✉) · D. Ramasamy · R.A. Bakar
Department of Mechanical Engineering, Universiti Malaysia Pahang, 26600 Pekan, Malaysia
e-mail: kumaran@ump.edu.my

K. Viswanatha Sharma and N. Hisham B Hamid (eds.),
Engineering Applications of Nanotechnology, Topics in Mining, Metallurgy and Materials Engineering, DOI 10.1007/978-3-319-29761-3_3

and the inlet temperature. Likewise, the simulation results show good agreement with the experimental data with deviation not more than 6 %. In addition, the SiO_2 nanofluid appears high values of the friction factor and heat transfer coefficient than TiO_2 nanofluid. Also, the base fluid (20 %EG + 80 %W) gives high values of the heat transfer coefficient and proper values of friction factor than other base fluids. It seems that the SiO_2 nanoparticles dispersed to (20 %EG + 80 %W) base fluid are a significant enhancement of the thermal properties than others. It is observed that the SiO_2 nanoparticles dispersed to (20 %EG + 80 %W) base fluid are a significant augmentation of heat transfer in the automobile radiator. The regression equations among input (Reynolds number, Prandtl number, and nanofluid volume concentration) and response (friction factor and Nusselt number) are found. The results of the analysis indicated a significant input parameters to enhance heat transfer with the automotive cooling system. The comparison between experimental results and other researchers' data is conducted, and there is a good agreement with a maximum deviation approximately 10 %.

Keywords Automotive · Cooling system · Nanofluid · Heat transfer

1 Introduction

The general definition of convection is the energy transfer between the surface and fluid due to temperature difference, and this energy transfer by either forced (external and internal flow) or natural convection. Forced convection is a mechanism or type of transport in which fluid motion is generated by an external source such as a fan, a pump, and a suction device. It should be considered as one of the main methods of useful heat transfer as significant amounts of heat energy can be transported very efficiently, and this mechanism is found very commonly in everyday life, including air-conditioning, central heating, steam turbines, and in many other machines. Forced convection is often encountered by engineers designing or analyzing heat exchangers, flow over a flat plate and pipe flow at a different temperature than the stream. The increasing demand for more efficient heat transfer fluids in many applications has led to enhance heat transfer to meet the cooling challenge necessary such as the photonics, transportation, electronics, and energy supply industries (Das et al. 2007). Conventional fluids nowadays are inherently poor heat transfer fluids and with the increasing demand of industries, micro-sized heat-generating systems are unable to provide adequate heat transfer. One of the possible solutions to this limited capability can be achieved by integrating the high heat transfer capability of solid metals into a flowing heat transfer fluid. In the past, attempts have been conducted to add micro-sized metal particles into conventional liquids, which ended with significant results as well as large disadvantages. Flow characteristics such as viscosity will change which led to the need to higher pumping power due to the addition of micro-particles. There is also a concern of agglomeration over time as well as corrosively of the system which can both result in high maintenance demands. The concept of nanofluids refers to a new

kind of heat transfer fluid formed by dispersing nano-scaled metallic or nonmetallic particles in base fluids (water, ethylene glycol, and oil). Energy transport of the nanofluid is affected by the properties and dimension of nanoparticles as well as a solid volume fraction. Some experimental investigations have revealed that the nanofluids have remarkably higher thermal conductivities than those of conventional pure fluids and have great potential for heat transfer enhancement. The addition of nano-sized particles is very proper to augment heat transfer as compared to the adding millimeter or micrometer sized to liquids with little penalty in pressure drop. A possible effective method for heat enhancement is to include high thermal conductivity particles in the liquid. Some general examples of applications that can benefit from this technology include home heating and cooling appliances, automotive radiator systems, power plant cooling systems, and computer processing cooling equipment, and more examples including heat are transferred from one medium to another. The use of high conductivity heat transfer materials will lead to benefit fully the available energy of a system which will reduce the environmental footprint of companies as well as their operating costs. It is believed that the most important reasons to enhance heat transfer of the nanofluids may be from the intensification of a turbulence eddy, repression, or interruption of the boundary layer as well as nanoparticles suspension. Therefore, the convective heat transfer coefficient of nanofluids is a function of properties, volume fraction of suspended nanoparticles, and dimension as well as the flow velocity. Taking advantage of the nanoparticles in the liquid causes the particles to stay in the solution for a long time. Another feature is that these particles have large surface area for thermal conductivity than ordinary liquids. From an engineering point of view, forced convection utilizing liquid coolants in laminar or turbulent flow regimes is always a key heat transfer solution. The better convective heat transfer performance means higher values of heat transfer coefficient. There are a number of techniques to enhance heat transfers such as modified heat transfer surface roughness, fins (extended surfaces), and injection. However, these techniques have led to higher pressure drop and hence lift pumping power requirement. Also, with low thermal conductivity and high viscosity of conventional heat transfer fluids such as water, ethylene glycol, oil, and ammonia, the convective thermal performance created barriers in designing small heat-rejecting devices. Therefore, an innovative coolant with improving heat transfer properties is required. The solid particles usually exhibit high thermal conductivity than liquids, and one approach to enhance thermal conductivity of liquids is by using suspensions, which contain dispersed particles into base fluids. One of the pioneering researchers of stationary, dilute dispersions of solid spheres has been studied by Ahuja (1975) performed number of tests on thermal conductivity and heat transfer coefficients of 40–100 μm-sized polystyrene–water-based solutions with 1-mm inside tube. Furthermore, the effective thermal conductivity of the suspension increases with the increasing of Reynolds number and nanofluid volume fraction. Because of shortage of available technology in those years, the particles size was large (in micro-scale). So this size has led to two penalties: The first on are not stable enough, and other are the larger particles can easily cause erosion to flow loop components.

1.1 Automotive Cooling System

Most internal combustion engines have used fluid coolant run through a heat exchanger (radiator) cooled by air. The water often used directly for the engine cooling, but there were obstacles as sedimentation may clog coolant passages, or salt may chemically damage the engine. Most engines' liquid for cooling has been used a mixture of water and chemicals such as antifreeze and rust inhibitors. The industrial term for the antifreeze mixture is engine coolant. Some antifreezes use no water at all, instead using a liquid with different properties, such as propylene glycol or ethylene glycol. Main requirement is that an engine fails if just one part overheats. Therefore, it is essential that the cooling system keeps all parts at properly low temperatures. Engine cooling systems are able to vary the size of their passageways through the engine block so that coolant flow may be adapted to the needs of each part. A typical four cylinder engine cruising along the highway at around 50 miles per hour will produce 4000 controlled explosions per minute inside the engine as the spark plugs ignite the fuel in each cylinder to propel the vehicle down the road. Clearly, these explosions produce an enormous amount of heat and, if not controlled, will destroy an engine in a matter of minutes. Controlling these high temperatures is the job of the cooling system. The radiator has been usually made of flattened aluminum or brass tubes with many fins on the external surface of tubes. These fins are capable of transferring heat from tubes into the airstream to be carried away from the vehicle. At the two ends of the radiator, there is a tank covers the ends of the radiator; in most of the cars, the tubes have run vertically with the tank on the top and bottom. On the back of the radiator on the side closest to the engine, there are one or two electrical fans inside a housing that is designed to direct the airflow. This fan is there to keep the airflow going through the radiator while the vehicle is going slow or is stopped while the engine is running. The engine temperature has been increased if this fan stops working, every time. The electrical fan is controlled by the vehicle's computer. A temperature sensor monitors engine temperature and sends this information to the computer. The computer determines whether the fan should be turned on and actuates the fan relay if additional airflow through the radiator is necessary. Another important device is the radiator pressure cap which will keep pressure in cooling system up to set point. The spring loaded valve when the pressure builds up higher than the set pressure point, calibrated to the correct Pascal (N/m^2), to release the pressure. Also, a small amount of fluid will bleed off if the cooling system pressure reaches the point to the cap needs till release this excess pressure. Since there is now less fluid in the system, as the engine cools down a partial vacuum has been formed. There is a secondary valve relates to the radiator cap to complete closed systems which allowed the vacuum in the cooling system to draw the fluid back into the radiator from the tank. Another simple device also keeps the fluid moving as long as the engine is running and this device is defined as a water pump. It is usually setup on the front of the engine and operates whenever the engine is working. The thermostat is a valve that controls the temperature of a fluid whenever hot weather enough, opens to allow the fluid to flow

through the radiator. And if the fluid is not hot enough, the flow to the radiator is blocked, and fluid is directed to bypass system that allows the coolant to return directly back to the engine. The bypass system allows the coolant to keep moving through the engine to balance the temperature and avoid hot spots. Because the flow to the radiator is blocked, the engine will reach operating temperature sooner and, on a cold day, will allow the heater to begin supplying hot air to the interior more quickly (Andrew 2008).

1.2 Nanofluid Synthesis Methods

A nanofluid may be synthesized by simply mixing nanoparticles dispersed to a liquid. In fact, the processes of synthesis are more involved. Metal oxide, carbon nanotube, nitride, carbide, and others nanoparticles may be readily purchased from the market. The reason to their side effective, these nanoparticles can normally be handled outside the boxes and other sealed containers during the preparation of the nanofluid. In order to break up the agglomerated particles and form a well-dispersed nanoparticle suspension, a stabilizing agent should add to avoid reagglomeration of the nanoparticles. In addition, the stabilizing agent affected the thermal properties, for instance, with altering the optical properties or viscosity of the nanoparticle solutions. Furthermore, the applicability of the nanofluid to the systems hinges on ability and real-life products to retain the small-sized character, and thus, for dispersing. Due to the high surface reactivity of the metal, it is reacting with the environment so nanofluids cannot be synthesized from pure solid metal nanoparticles. The single-step methods for the nanofluid synthesized with a limit agglomeration as reported by Das et al. (2007). Over the years, a few processes have been developed for the direct nanofluid synthesis. The metal salt solutions are reduced to a stabilizing agent, and the small particles form sediment. There are also a number of plasma synthesis approaches: Metal oxide, nitride, or carbide nanoparticles may be synthesized by condensation/evaporation with the nitrogen, oxygen, or a light hydrocarbon. The main advantages of the plasma synthesis processes are the possibility to synthesize complex chemical compositions and structures, in situ stabilization, and scalability. The nanoparticles in a host fluid interact strongly with van der Waals interactions because of the large surface area of the nanofluid and incessant solid–solid collisions due to Brownian effect. Undesirably, particle collision can lead the agglomeration process whereby large, sometimes up to micron-sized, particles are produced. Due to the weight, such particles cannot be maintained in suspension by Brownian moving and settle out of dispersions. In applications where the fluid is pumped through conduits, this process also leads to abrasion of conduit walls. In the agglomeration process, soft and hard agglomerates may form. Soft agglomerates may be broken up by sonication which means of fluid agitation. Hard agglomerates, however, which are associated with nanoparticle sintering, cannot be broken up by simple means. In the last years, many attempts have been made to make stable nanofluids with partial success.

Various methods have been used to stabilize the nanoparticle suspension. Some rely on electrostatic repulsion where the nanoparticles acquire surface charges once in solution forming an electrical double layer. The hydrophilic end of the compound ensures compatibility with a polar solvent. Chemical functionalization of the nanoparticle surface can also be used to cause particles to favor interactions with the host liquid. Using surfactants has been wide-spread across the nanofluid applications though their usefulness is somewhat overshadowed by its limitations. One well-known issue is the irreversible deterioration of the surfactant at rather modest temperatures. Typically, surfactants degrade significantly above 60 °C.

1.3 Nanofluid Applications

One of the major advantages of going to a system that uses nanoparticle suspensions is the operating mode of the system. Small changes of these fields can change scattering and absorption. The first one using particles in the solar collector was who mixed particles in a gas-working fluid. In years following, gas particle receivers have been extensively modeled, and several prototype collectors have been built and tested. The researchers experimentally illustrate the absorption of radiation using nanoparticles and have been done by the following: (Abdelrahman et al. 1979). Although the researchers used particles mixed with a gas (not liquids), there are a few recent studies that have been used the concept of liquid-based nanofluid experimentally in the solar collectors. Their experimental results showed that the volume fraction of nanoparticles can achieve the incoming light to be absorbed in a thin surface layer where the thermal energy was easily lost to the environment. The regime map of the solar absorbing nanofluids in comparison with other common particulate mediums has been reported.

1.3.1 The Big Impact of Nanoparticles

What does the future hold for nanofluids? Although there still exist a growing number of publications in the field of nanofluids, one has to be concerned with the funding trends going forward, particularly in the thermal transport community. After detection of the last ten years, the nanofluid researches peaked in 2007 and have been increasing since. On the other hand, with so many emerging, exciting applications (i.e., excluding conductive/convective studies), we believe nanofluids will have a big impact for some time to come.

2 Forced Convection in a Car Radiator

There are many different applications of thermal fluid systems, including automotive cooling systems. Base fluids, such as water, ethylene glycol, and glycerol, have been used as conventional coolants in automobile radiators for many years; however, these fluids have low thermal conductivities. The low thermal conductivities have thus prompted researchers to search for fluids with high thermal conductivities than that of conventional coolants. Therefore, nanofluids have been used instead of the commonly used base fluids.

(i) ***Experimental studies***

Investigated forced convection heat transfer to reduce circulating water in an automobile radiator.

The effects of different amounts of Al_2O_3 nanoparticles on the heat transfer performance of an automobile radiator were determined experimentally as shown in Fig. 1. The range of flowrates was varied between 2 and 6 LPM with a changing fluid inlet temperature for all experiments. The results showed that the enhancement of heat transfer using nanofluids is 40 % compared with using water.

Forced convection heat transfer of both CuO and Fe_2O_3 nanofluids flow through the car radiator has presented by Peyghambarzadeh et al. (2013). The overall heat transfer coefficient (U) according to the conventional 3-NTU technique has been evaluated to find the performance of heat transfer as shown in Fig. 2. Three volume fractions 0.15, 0.4, and 0.65 % have been added to water to prepare nanofluids. The range of Reynolds number is 50–1000, and the inlet liquid temperature is changed

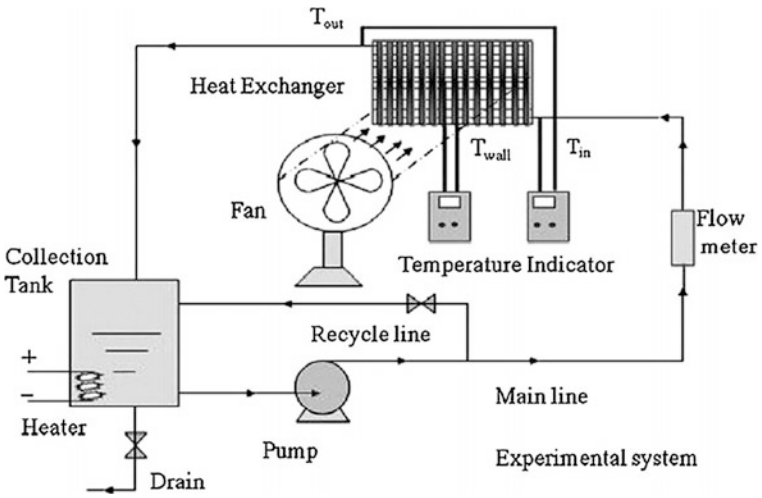

Fig. 1 Test rig in the experimental work. *Source* Peyghambarzadeh et al. (2011)

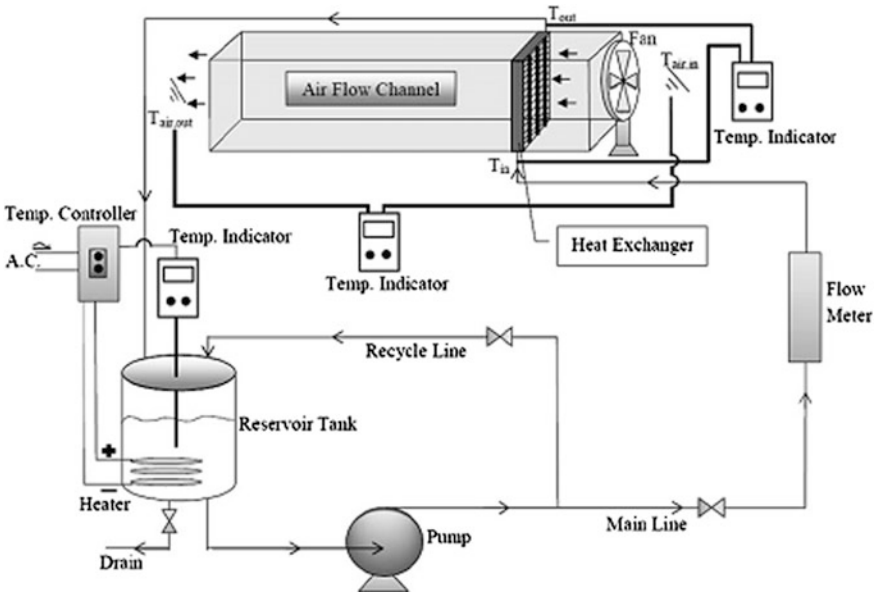

Fig. 2 Cooling loop setup of automobile cooling system. *Source* Peyghambarzadeh et al. (2013)

to 50, 65 and 80 °C. Results showed that both nanofluids appear greater overall heat transfer coefficient as compared to water up to 9 %. Furthermore, increasing the nanoparticle concentration, air velocity, and nanofluid velocity enhances the heat transfer coefficient.

(ii) ***Numerical studies***

A numerical study analyzed mixed convective flows through a U-shaped grooved tube in a radiator has been conducted. The enhanced heat transfer of an automobile radiator was investigated with properties of the nanofluid as input data. It appeared that the heat transfer coefficient and heat transfer rate in the engine cooling system increased using copper–ethylene glycol nanofluids compared with using pure ethylene glycol. The results showed that the addition of 2 % copper particles in ethylene glycol achieved a result of 3.8 % better compared with using pure ethylene glycol at air and coolant Reynolds number of 6000 and 5000, respectively. The influence of the working conditions on both fluids (mass flow and inlet temperature) and the impact of the selected coolant fluid in a car radiator were investigated numerically by Oliet et al. (2007). The application of a copper–ethylene glycol nanofluid in a car cooling system was studied. Several geometrical parameters (fin pitch and louver angle) and the importance of the coolant flow layout on the radiator global performance were analyzed. The results showed that the use of this numerical model as a rating and design tool for car radiator manufacturers is a reasonable compromise between the NTU and the CFD methods. A numerical study on laminar heat transfer using CuO and Al_2O_3-ethylene glycol

and water inside a flat tube of a car radiator was performed. A modified SIMPLE algorithm for the irregular geometry was developed to determine the flow and temperature field. The results have been used as a fundamental data for the tube design by suggesting optimal specifications for radiator tubes. Two liquids, water and ethylene glycol/water mixture, used as the coolant fluid in a meso-channel heat exchanger were studied numerically. The predicted results (heat transfer rate, pressure, and temperature drops in the coolants) from the numerical simulation were compared with the experimental data for the same geometrical and operating conditions and showed good agreement. Additionally, the results showed the heat exchanger was enhanced, with heat transfer rate approximately 20 % greater than that of a straight slab of the same length; the enhanced heat exchanger has a good potential to be used as a car radiator with reasonably enhanced heat transfer characteristics using an ethylene glycol/water mixture as the coolant. Different types of nanoparticles (copper, diamond, and silicon dioxide) in ethylene glycol in automotive flat tube plate-fin cross-flow compact heat exchangers (CHEs) were investigated numerically. The volume concentration for all nanofluid types used was 2 %. The three-dimensional governing equations were solved with the finite volume method using the k-• turbulence model with Reynolds numbers ranging from 4000 to 7000. The nanofluids used in the compact heat exchangers results in more energy transfer and are more cost-effective than conventional coolants. A CFD model of the mass flowrate of air passing across the tubes of a car radiator was introduced. The airflow was simulated using the commercial software ANSYS 12.1, where the geometry was created in the software SOLIDWORKS, followed by creating both the surface mesh and the volume mesh accordingly. The results were compared and verified according to the known physical situation and existing experimental data. The results serve as a good database for future investigations.

2.1 Outlook

Regarding all these experimental studies of the heat transfer fluid flow may be enhanced when suspended small solid particles less than 100 nm diameter of a metal or non-metallic on fluids with a little percentage of volume fraction. On the other side, noted from all these investigations of numerical studies is to enhance heat transfer in fluid through circular tube and heat exchanger using simulation commercial software. The studies of heat transfer nanofluids in a car radiator are limited. The experimental researches of heat transfer nanofluid in an automotive radiator have been conducted with CuO, Al_2O_3, and Fe_2O_3 with volume concentration not more than 1 % and Reynolds number in the range less than 1000. Likewise, the numerical studies of nanofluid heat transfer in a car radiator were in the laminar flow condition, and volume fractions were less than 2 %.

3 Experimental Work

The heat transfer performance of liquids is limited by their poor thermophysical properties compared with that of solids, which is the primary reason behind adding solid particles less than 100 nm in diameter to a fluid, i.e., to improve the thermal properties of the fluid; this new type of fluid is called a nanofluid. Dispersing solidly metallic or non-metallic materials in a base fluid (liquid), such as water, ethylene glycol, and glycerol, has become an interesting topic in recent years (Buongiorno 2006; Abbasian and Amani 2012; Bozorgan et al. 2012). There are many different applications of thermal fluid systems, including automotive cooling systems. Base fluids, such as water, ethylene glycol, and glycerol, have been used as traditional coolants in automobile radiators for many years; however, these fluids have low thermal conductivities. The low thermal conductivities have thus prompted researchers to search for fluids with higher thermal conductivities than that of conventional coolants. Therefore, nanofluids have been used instead of the commonly used base fluids.

In this chapter, the first part of methodology is the experimental work which contained the preparation of nanofluids and thermal properties measurement, the experimental test rig setup with all devices and also, the data analysis and uncertainty calculations are conducted. Another part is the CFD analysis which included the grid independent test and the simulation results of the heat transfer nanofluid through the flat tube of the radiator.

3.1 Nanofluid Preparation

The VEROS method (Akoh et al. 1978) to prepare nanofluid has been conducted which contained dispersing nanoparticles into base fluids (pure water, EG, and Water/EG). Nanofluids are prepared in the thermal laboratory of mechanical engineering faculty University Malaysia Pahang. Deionized water was prepared in the laboratory by double distillation before using it for the experiments as shown in Fig. 3a. The nanopowders as shown in Fig. 3b have been purchased from the US Research Nanomaterial's, Inc. (NovaScientific Resources (M) Sdn. Bhd). On the other side, the ethylene glycol was already purchased with nanoparticles.

Mechanical stirrers have been applied to be a homogeneous mixture for at least one hour as shown in Fig. 4a. An ultrasonic process has been done for two hours approximately to break up any residual agglomerations as shown in Fig. 4b.

The volumetric ratio of 10 % and 20 % of EG is added to the deionized water to prepare other base fluids (10 %EG-90 %water) and (20 %EG-80 %water). The reason to make these types of base fluids is to find the optimum base fluid has the highest ability of heat transfer enhancement.

(a) Distillation of water (b) the nanopowders

Fig. 3 Base fluid and nanopowders used in the experiment

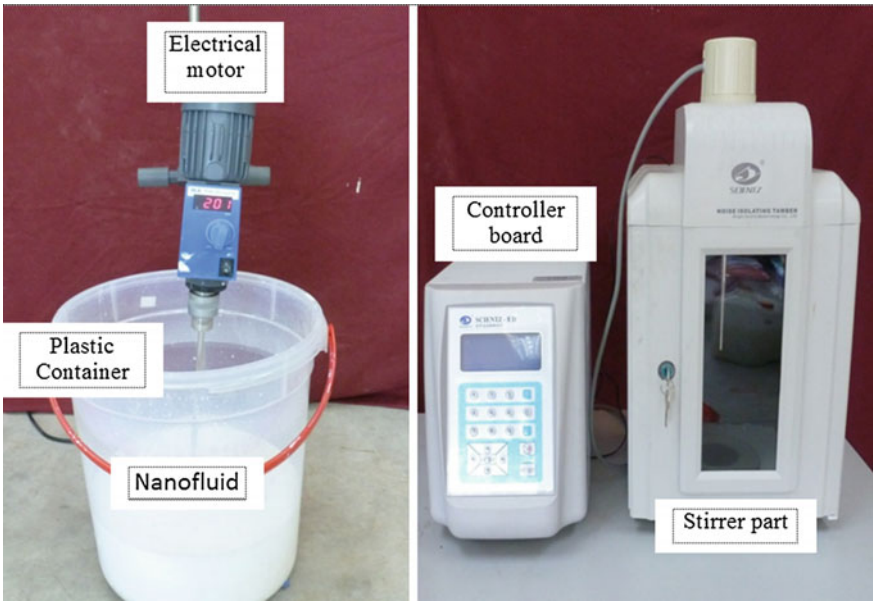

(a) Mechanical stirrer (b) Ultrasonic stirrer

Fig. 4 Stirrers' apparatus

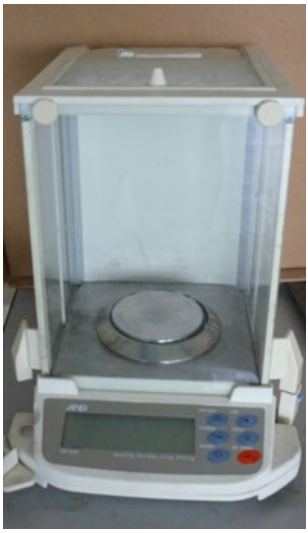

Fig. 5 Laboratory balance

Measured quantities of TiO_2 and SiO_2 nanoparticles were suspended a base fluid (pure water, pure EG, 10 %EG-90 %water, and 20 %EG-80 %water) to obtain mass concentration φ. The mass of nanoparticles (m_p) and base fluid (m_f) has been measured by weighing measurement with accuracy ($\pm 0.0001g$) as shown in Fig. 5.

To find the weight percentage (φ), Eq. (3.1) has been used as:

$$\varphi = \left(\frac{m_p}{m_p + m_f}\right) \times 100 \tag{3.1}$$

To estimate the volume concentration of nanofluid $\emptyset$ depending on nanoparticles density $\left(\rho_p = \frac{m_p}{\rho_p}\right)$ and base fluid density $\left(\rho_f = \frac{m_f}{\rho_f}\right)$ at 25 °C, Eq. (3.2) was used as:

$$\emptyset = \frac{\rho_p}{\rho_p + \rho_f} \tag{3.2}$$

The nanofluid volume concentrations desired in the study undertaken are (1–4) % Table 1.

3.1.1 Experimental Test Rig Setup

The test rig shown in Fig. 6 has been used to measure the friction factor and heat transfer coefficient in the automotive engine radiator. This experimental test rig setup has included:

Table 1 Thermal properties of nanoparticle and base fluids at 25 °C

Materials	Density (Kg/m^3)	Specific heat (J/Kg. °C)	Thermal conductivity (W/m. °C)	Viscosity (Pa. s)
SiO_2	2220	703	1.2	–
TiO_2	4175	692	8.4	–
Pure water	992	4174	0.633	0.00065
EG	1101	2382	0.256	0.0095
10 % EG-90 % Water	1002	4090	0.59	0.00165
20 % EG-80 % water	1006	4024	0.57	0.00188

Source, ASHRAE (2005)

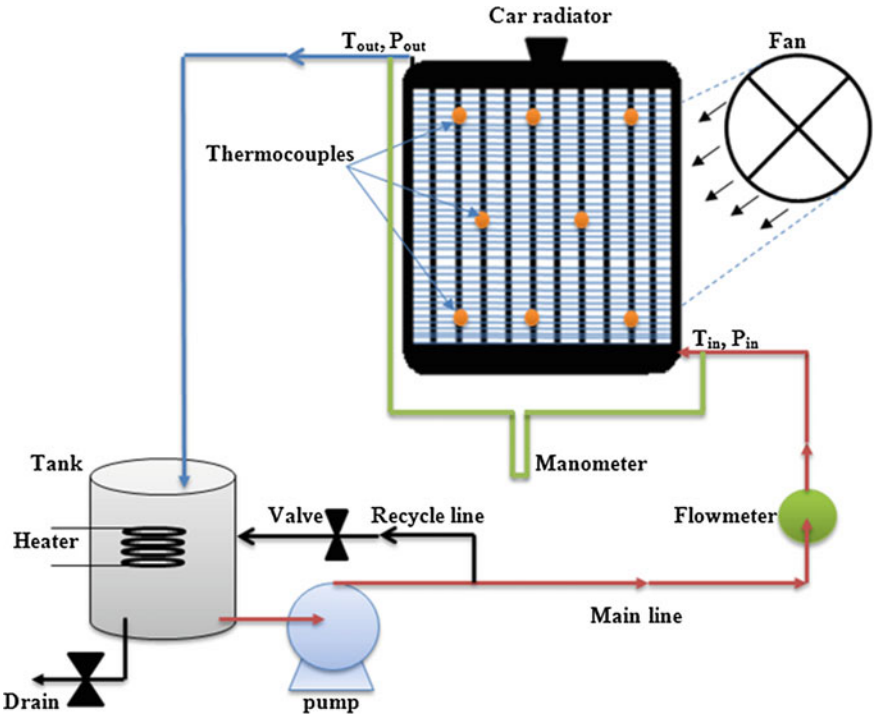

Fig. 6 Experimental test rig setup

The car radiator is shown in Fig. 7 which contained inlet and outlet gap with 0.75*in* and 32 flat tubes with major and minor dimensions as ($D = 9\ mm$) and ($d = 3\ mm$), respectively. Fins plates with 1 mm thickness and brass material have been inherent with the tubes. The equally spaced 1 mm among the fins has been

Fig. 7 Car radiator

fabricated to flow air inside it. The coolant fluid flows through the inlet gap to the 32 flat tubes from the bottom to the top and then exits from the outlet gap of radiator. The air-side fins are flowing horizontally to cool the surface wall.

3.1.2 Experimental Procedure

The nanofluid is directly pumped through the test section of the apparatus. At the first, there was a high vibration in the system till steady state at that time no vibration and flow with keeping quite. To ensure the radiator filling with the fluid, the outlet point should be up to level than radiator level as shown in Fig. 6. The valves have been opened to allow the nanofluid flowing through the pipes and control the velocity of flow. The two-pass flow had been found to allow the pump in the rest and did not press. The apparatus tubing was a major factor in the reliability of the results of the experiments. The first factor that was supposed when looking at the tubing selection was the material of which they were made. Ideally, the material would be chosen to have as little heat transfer resistance as possible. This would help to reduce error as it would help raise the overall heat transfer, and, therefore, that heat transfer would be measured with far higher accuracy. However, in this real-world experimental apparatus, other factors affected the selection. Considering the nanofluids contained solid particles, these particles have a tendency to agglomerate and sediment that would lead to clog in the tubes. This makes it difficult to use metallic tubes, perfect for high heat transfer rates, and suggests that perhaps a rubber or soft plastic tube for more perfect in order to break these clogs loose without affecting the experiment. The abrasiveness of the flowing nanofluid was also considered. This could cause erosion damage to a softer material and would most likely mean that the testing section would regularly have to be replaced if one of these softer materials has been used. Also, a factor that likely has a minimal effect on the convection coefficient but still may need to be considered is a

contact resistance. This is because the solid particles in the nanofluid may experience a resistance due to imperfect contact as occurs in nearly all solid-to-solid heat transfer, and this resistance could vary based on the material that of which the tubing is made. The second factor for tubing has been considered is the tube diameter. This factor had to differ as it helped change flowrate and velocity. Also, the diameter has been employed by the definition of Nusselt number. The difference did not have to be extremely large, but some variation was needed. The final decision on the using tube was based on all of these factors. The tubing used was all plastic at different sizes. The sizes were based on traditional inner diameter standards of a $1/2in$ and $3/4in$. The material was chosen as to resist as much abrasion from the nanoparticles as possible. The sizes were selected to balance the necessary variation with the need to be able to alter the Reynolds Number as many as possible with the pump flowrate restrictions.

The following parameters should measure to determine the heat transfer coefficient at various flow conditions: flowrate, pressure drop, and fluid temperature in and out of the car radiator, the wall temperature of the car radiator, and the heater voltage and current. All data collected have been first handwritten and then copied into Excel so that a hard copy of the data was kept for record. This reduced the risk of errors associated with simply typing raw data into Excel and provided a hard copy of the data to be preserved. Depending on the status of the loop, any number of procedures may be required before collecting data. If starting with a new fluid and cleaning apparatus, the filling procedure must be run to charge the system. If the system were already charged at the start of the test, then only the start-up procedure was run. Once these preliminary steps had been accomplished, the pump and heaters were started to begin collecting data. Each run consisted of the temperature, flowrate, pressure, and heat input data for a minimum of 5 individual process flowrates. It was decided early on that at least five flowrates were necessary for each fluid in order to determine any trends. For all tests, the heating power was held constant, and the process flowrate has been varied. The volumetric flowrate range of 1-5 LPM for water and 3-12 LPM for other base fluids has been tested. Given its poor heat transfer properties, EG could not be run at flowrates below 2 LPM due to overheating and the flow keep it slowly and laminar along experiments. The steady-state operation should be conducted for convective heat transfer coefficient calculations. The system has been taken approximately 20 min to reach steady operating conditions. At the beginning with the lowest flowrate, data were obtained at steady-state conditions. The flowrate was then increased by a small amount, and the system was allowed to return to steady state. For keeping the constant inlet temperature, the voltage regulator should provide the heater with proper voltage and keeping at this point. Then, changing of the voltage will lead to change the inlet temperature. Typically, the system took 15–20 min to return to steady state after the increasing flowrate manner. Once the inlet temperature set point was reached, the data were once again obtained. This procedure was repeated up to the maximum flowrate. The nanofluid volume concentration has been changed then repeating all these procedures.

3.1.3 Experimental Data Analysis

According to Newton's cooling law, the following procedure followed to obtain heat transfer coefficient and corresponding Nusselt number as (Bejan 2004) is as follows:

$$Q_c = hA\Delta T = hA_s(T_b - T_s) \tag{3.7}$$

A_s is the surface area of the tube, and T_b is the bulk temperature

$$T_b = \frac{T_{\text{in}} + T_{\text{out}}}{2} \tag{3.8}$$

(T_{in}, T_{out}) are the inlet and outlet temperatures and T_s is the tube wall temperature which is the mean value of two surface thermocouples as:

$$T_s = \frac{1}{a}\sum_{i=1}^{a} T_i \tag{3.9}$$

And heat transfer rate calculated by:

$$Q_c = \dot{m}C\Delta T = \dot{m}C(T_{\text{in}} - T_{\text{out}}) \tag{3.10}$$

$\dot{m}$ is the mass flowrate which is determined as:

$$\dot{m} = \rho \times \dot{V} \tag{3.11}$$

The electrical power supplied to provide the system with heat by electrical heater has been calculated as:

$$\not{P} = I \times E \tag{3.12}$$

where I and E are the current and the voltages, respectively, have been measured directly from the voltage regular.

The heat rejected (Q_{rej}) outside the system has been calculated as follows:

$$Q_{\text{rej}} = \not{P} - Q_c \tag{3.13}$$

The heat transfer coefficient can be evaluated by collecting Eq. (3.7) and Eq. (3.10):

$$h = \frac{\dot{m}C(T_{in} - T_{out})}{nA_s(T_b - T_s)} \tag{3.14}$$

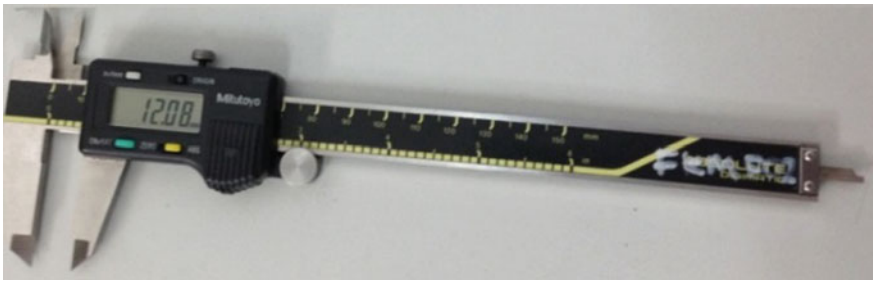

Fig. 8 Digital clipper

where n is the tubes number of the radiator. Then Nusselt number can be also calculated as:

$$Nu = \frac{h \times D_h}{k} \tag{3.15}$$

D_h is the hydraulic diameter of the tube which is estimated by describing the problem undertaken as cylindrical geometry coordinates. Dimensions of the flat tube are major and minor diameters ($D = 9\ mm$, $d = 3\ mm$) have been measured by using digital clipper as shown in Fig. 8. The length (L) and hydraulic diameter (D_h) of the flat tube are 345 and 4.68 mm, respectively. The Reynolds number calculated regarding hydraulic diameter (D_h) is as follows:

$$D_h = \frac{4 \times \left[\frac{\pi}{4} d^2 + (D - d) \times d\right]}{\pi \times d + 2 \times (D - d)} \tag{3.16}$$

Assume all thermal properties have estimated at the bulk temperature of the fluid.

Reynolds number (Re) is determined as:

$$Re = \frac{4\dot{m}}{\pi D_h \mu} \tag{3.17}$$

u is the velocity at inlet radiator which is evaluated from volumetric flowrate $(\dot{V})$ and the cross-sectional area of tube (A_{cross}) as:

$$u = \frac{\dot{V}}{nA_{cross}} \tag{3.18}$$

The friction factor (f) can be calculated depending pressure drop $(\bullet P)$ reading from manometer as:

Table 2 Uncertainty analysis for data measured

Quantity	Uncertainty	Unit
Tube length	±1.5712	mm
Hydraulic diameter	±0.0072	mm
Surface area	±0.7669	mm^2
Cross-sectional area	±0.055	mm^2
Temperature	±0.1	°C
Pressure	±0.133416	N/m^2
Density	±2.0	kg/m^3
Specific heat capacity	±4.0	J/kg.°C
Thermal conductivity	±0.05	W/m.°C
Viscosity	±0.0004	N. s/m^2
Velocity	±0.0087	m/s
Flowrate	±0.5	m^3/s
Power	±0.51	W
Coolant heat transfer	±1.3323	W
Heat transfer rejected	±1.3433	W
Heat transfer coefficient	±5.4225	W/m^2. °C
Nusselt number	±0.22	_
Reynolds number	±3.456	_

$$\Delta P = S \times g \times H \tag{3.19}$$

$$f = \frac{2 \times \Delta P}{\frac{L}{D} \times \rho \times u^2} \tag{3.20}$$

3.1.4 Uncertainty Analysis

The uncertainty analysis has been performed by calculating the measurement error as shown in detail in Appendix B. According to uncertainty analysis described, the error measurement of the parameters is summarized in Table 2. Furthermore, to check the reproducibility of the experiments, some runs were repeated later which proved to be excellent.

4 Result and Discussion

4.1 Outlet Temperature

The outlet temperature after the heat transfer across the radiator has been measured by connecting a thermocouple sensor at the exit point of the test rig as outlined in Chapter 3. In order to consider the influence of the temperature on heat transfer of

the car radiator, different inlet temperatures of the nanofluids have been applied. It is important to mention that from a practical viewpoint for every cooling system, at equal mass flowrate the more reduction in working fluid temperature indicates a better thermal performance of the cooling system Peyghambarzadeh et al. (2011). Figure 9 shows the outlet temperature at the volume flowrate range (1–5) LPM with the range of the inlet temperature (60, 70, and 80 °C). It seems the outlet temperature increases with the increasing of the volume flowrate. Figure 9a indicates the outlet temperature increases by 17 % for TiO_2 suspended to water with increase of volume flowrate at different inlet temperatures. On the other side, at fixed flowrate the outlet temperature decreases by 8 % when the volume fraction increases from 1 to 4 %. Likewise, the pure water appears high outlet temperature as compared to the nanofluid. This behavior refers to the increase of heat transfer across the system when adding solid nanoparticles to the liquid. Figure 9b shows also the outlet temperature increases by 17 % for SiO_2 dispersed to water with increase of volume flowrate at different inlet temperature. It seems the outlet temperature values of SiO_2 nanofluid are lower than the values of TiO_2 nanofluid.

It should be said the SiO_2 nanofluid is better than TiO_2 nanofluid for heat transfer enhancement. Figure 10a illustrates the outlet temperature increases by 11 % for TiO_2 suspended to EG with increase of the volume flowrate from 2 LPM to 12 LPM at different inlet temperatures. Furthermore, at fixed flowrate the outlet temperature decreases by 6 % when the volume fraction increases from 1 % to 4 %. Likewise, the pure EG gives high outlet temperature as compared to the nanofluid. Figure 10b indicates also the outlet temperature increases by 11 % for SiO_2 dispersed to EG with increase of volume flowrate at different inlet temperatures. It observes the outlet temperature values of SiO_2 nanofluid are lower than the values of TiO_2 nanofluid. In the same manner should be said the SiO_2 nanofluid is better than TiO_2 nanofluid for heat transfer enhancement. Figure 11a demonstrates the

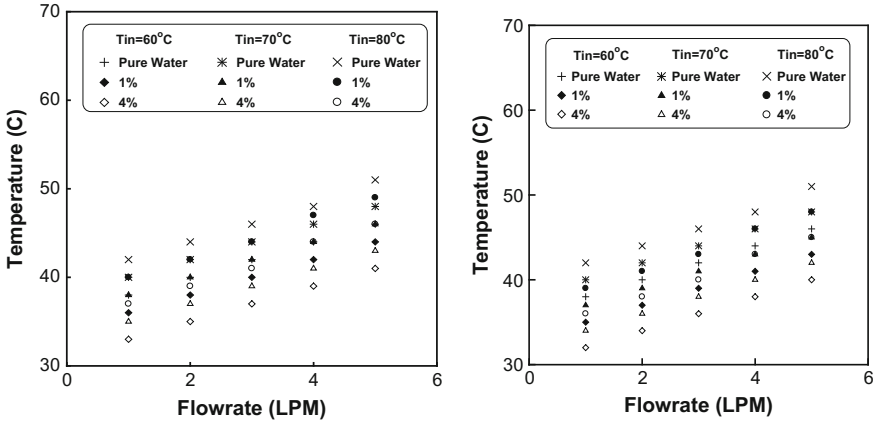

(a) TiO_2-Water (b) SiO_2-Water

Fig. 9 Outlet temperature at different flowrate for nanoparticles suspended to water as a base fluid

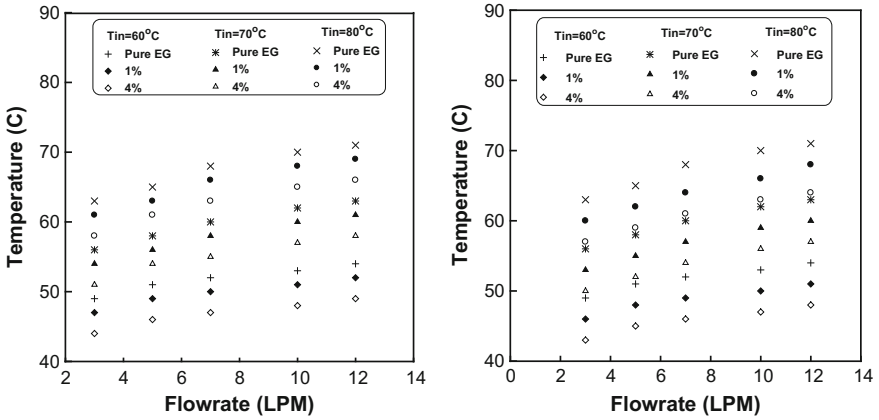

Fig. 10 Outlet temperature at different flowrate for nanoparticles suspended to EG as a base fluid

outlet temperature increases by 10 % for TiO_2 suspended to 10 %EG + 90 %W with increase of the volume flowrate at different inlet temperature. Furthermore, at fixed flowrate the outlet temperature decreases by 6 % when the volume fraction increases from 1 to 4 %. Likewise, the pure 10 %EG + 90 %W gives high outlet temperature as compared to the nanofluid. Figure 11b indicates also the outlet temperature increases by 11 % for SiO_2 dispersed to 10 %EG + 90 %W with increase of volume flowrate at different inlet temperatures. It observes the outlet temperature values of SiO_2 nanofluid are lower than the values of TiO_2 nanofluid. In the same manner should be said the SiO_2 nanofluid is better than TiO_2 nanofluid for heat transfer enhancement.

Figure 12a illustrates the outlet temperature increases by 7 % for TiO_2 suspended to 20 %EG + 80 %W with increase of the volume flowrate at different inlet temperatures. Furthermore, at fixed flowrate the outlet temperature decreases by 7 % when the volume fraction increases from 1 to 4 %. Likewise, the pure 20 % EG + 80 %W gives high outlet temperature as compared to the nanofluid. Figure 12b indicates also the outlet temperature increases by 11 % for SiO_2 dispersed to 20 %EG + 80 %W with increase of volume flowrate at different inlet temperatures. It observes the outlet temperature values of SiO_2 nanofluid are lower than the values of TiO_2 nanofluid. In the same manner should be said the SiO_2 nanofluid is better than TiO_2 nanofluid for heat transfer enhancement.

4.2 Heat Transfer

The heat transfer inside the flat tube of the radiator is represented the coolant heat transfer which is plotted in Fig. 13.

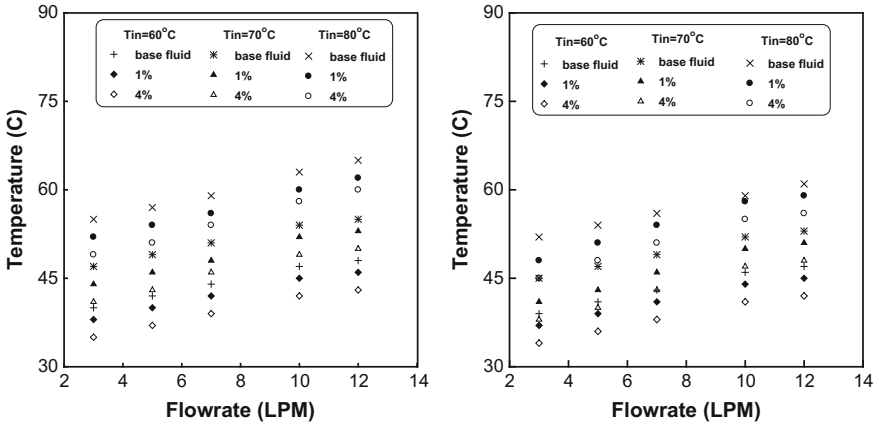

(a) TiO_2-10%EG+90%W (b) SiO_2-10%EG+90%W

Fig. 11 Outlet temperature at different flowrate for nanoparticles suspended to 10 %EG + 90 % W as a base fluid

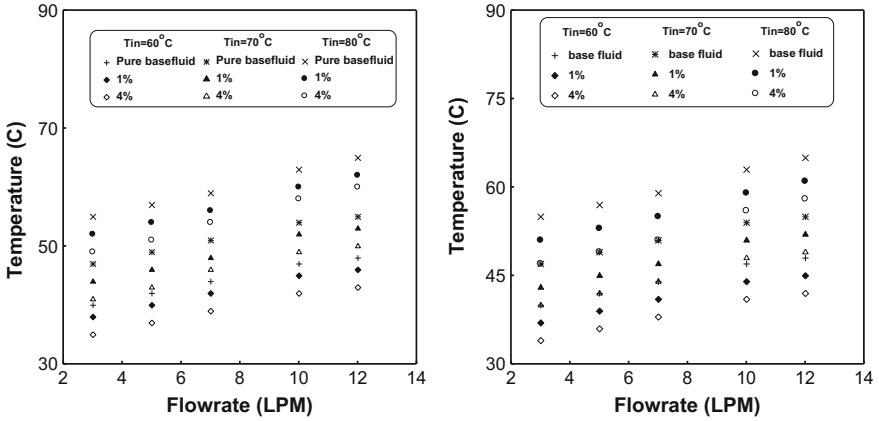

(a) TiO_2-20%EG+80%W (b) SiO_2-20%EG+80%W

Fig. 12 Outlet temperature at different flowrate for nanoparticles suspended to 20 %EG + 80 % W as a base fluid

The coolant heat transfer at the range of the volume flowrate from 1 LPM to 5 LPM for TiO_2 suspended to water is indicated in Fig. 13a. It can be observed the coolant heat transfer increases from 53 to 178 W and 62 to 218 W for 1 and 4 % of TiO_2-water at 60 °C. It can be seen, at 1 LPM volume flowrate the coolant heat transfer increases from 53 W at 60 °C to 89 W at 80 °C. On the other hand, at 5 LPM volume flowrate the coolant heat transfer increases from 178 W at 60 °C to 384 W at 80 °C for 1 % TiO_2-water. This means the increasing percentage of the

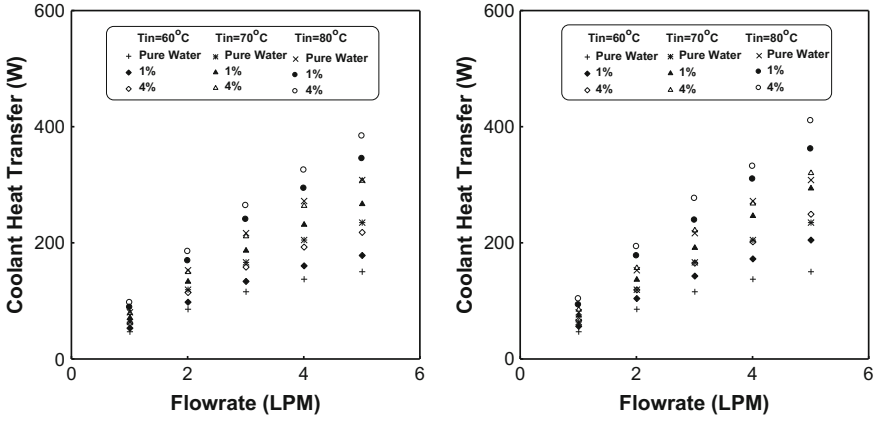

Fig. 13 Coolant heat transfer at different flowrate for nanoparticles suspended to water as a base fluid

coolant heat transfer is 13 % and 75 % at the volume flowrate from 1 LPM to 5 LPM, respectively. Figure 13b shows the coolant heat transfer increases from 56 to 205 W for 1 % SiO_2 suspended in water at 60 °C. However, the increasing of the cooling heat transfer is from 66 to 249 W for 4 % volume fraction of SiO_2-water. Likewise, at 80 °C the coolant heat transfer increases from 93 to 361 W. Figure 14a shows the coolant heat transfer at the range of the volume flowrate from 3 LPM to 12 LPM for TiO_2 suspended to EG. It can be seen the coolant heat transfer increases from 52 to 128 W and 70 to 160 W for 1 % and 4 % of TiO_2-water at 60 °C. It can be noted at 3 LPM volume flowrate the coolant heat transfer increases from 52 W at 60 °C to 75 W at 80 °C.

On the other hand, at 12 LPM volume flowrate the coolant heat transfer increases from 128 W at 60 °C to 175 W at 80 °C for 1 % TiO_2-water. This means the increasing percentage of the coolant heat transfer is 13 and 75 % at the volume flowrate from 1 LPM to 5 LPM, respectively. Figure 14b shows the coolant heat transfer increases from 62 to 159 W for 1 % SiO_2 suspended in water at 60 °C. However, the increasing of the cooling heat transfer is from 75 to 214 W for 4 % volume fraction of SiO_2-water. Likewise, at 80 °C the coolant heat transfer increases from 88 to 211 W. Figure 15a shows the coolant heat transfer at the range of the volume flowrate from 3 LPM to 12 LPM for TiO_2 suspended 10 % EG + 90 %W. It can be seen the coolant heat transfer increases from 143 to 366 W and 165 to 450 W for 1 % and 4 % of TiO_2-10 %EG + 90 %W at 60 °C.

It can be noted at 3 LPM volume flowrate the coolant heat transfer increases from 143 W at 60 °C to 194 W at 80 °C. On the other hand, at 12 LPM volume flowrate the coolant heat transfer increases from 366 W at 60 °C to 518 W at 80 °C for 1 % TiO_2-10 %EG + 90 %W. This means the increasing percentage of the coolant heat transfer is 25 and 40 % at the volume flowrate from 3 LPM to 12 LPM,

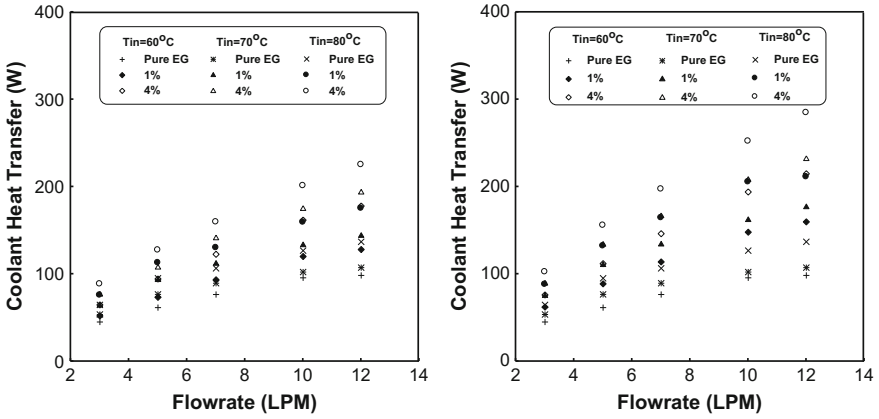

(a) TiO_2-EG (b) SiO_2-EG

Fig. 14 Coolant heat transfer at different flowrate for nanoparticles suspended to water as a base fluid

respectively. Figure 15b shows the coolant heat transfer increases from 158 to 413 W for 1 % SiO_2 suspended in 10 %EG + 90 %W at 60 °C. However, the increasing of the cooling heat transfer is from 183 to 507 W for 4 % volume fraction of SiO_2-10 %EG + 90 %W. Likewise, at 80 °C the coolant heat transfer increases from 218 to 574 W.

Figure 16a indicates the coolant heat transfer at the range of the volume flowrate from 3 LPM to 12 LPM for TiO_2 suspended to 20 %EG + 80 %W. It can be seen the coolant heat transfer increases from 143 to 365 W and 167 to 455 W for 1 %

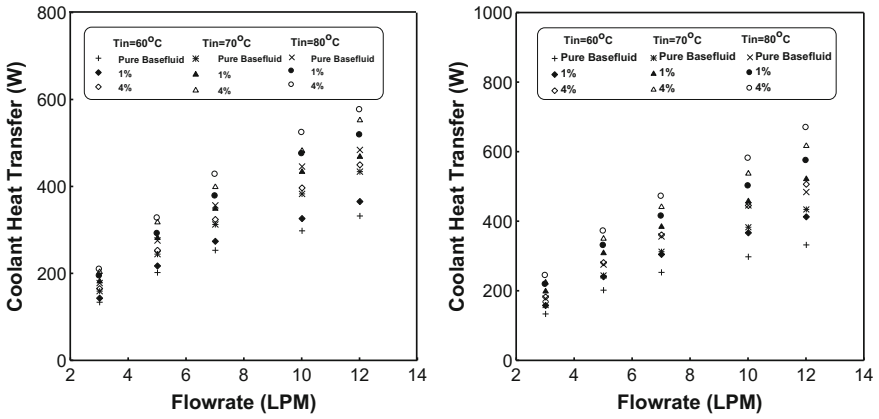

(a) TiO_2-10%EG+90%W (b) SiO_2-10%EG+90%W

Fig. 15 Coolant heat transfer at different flowrate for nanoparticles suspended to 10 % EG + 90 %W as a base fluid

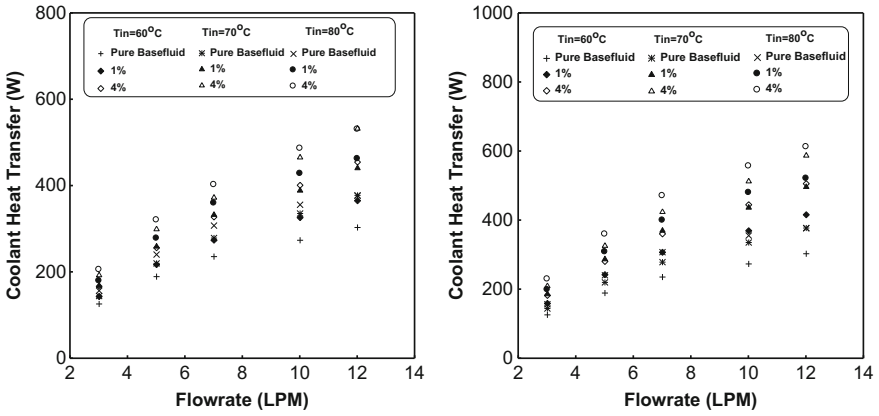

Fig. 16 Coolant heat transfer at different flowrate for nanoparticles suspended to 20 % EG + 80 %W as a base fluid

and 4 % of TiO_2-20 %EG + 80 %W at 60 °C. It can be noted at 3 LPM volume flowrate the coolant heat transfer increases from 143 W at 60 °C to 179 W at 80 °C. On the other hand, at 12 LPM volume flowrate the coolant heat transfer increases from 365 W at 60 °C to 462 W at 80 °C for 1 % TiO_2-20 %EG + 80 % W. This means the increasing percentage of the coolant heat transfer is 51 and 57 % at the volume flowrate from 3 LPM to 12 LPM, respectively.

Figure 16b shows the coolant heat transfer increases from 159 to 416 W for 1 % SiO_2 suspended in 20 %EG + 80 %W at 60 °C. However, the increasing of the cooling heat transfer is from 182 to 506 W for 4 % volume fraction of SiO_2-20 % EG + 80 %W. Likewise, at 80 °C the coolant heat transfer increases from 199 to 521 W.

4.3 Heat Rejected

The heat leaved the radiator from the air side is now the heat rejected. Figures 17, 18, 19, and 20 show the heat rejected from the system at different volume flowrate. It can be seen the effect of the volume concentration and the inlet temperature on the heat rejected. Figure 17a indicates the heat rejected decreases from 646 W and 637 W to 521 W and 480 w for both 1 % and 4 % TiO_2-water from 1 LPM to 5 LPM at 60 °C. It seems the increasing in the inlet temperature caused to decrease in the heat rejected by 32 %. However, the increase in the volume fraction is due to decrease in the heat rejected by 4 %. Figure 17b shows the heat rejected decreases from 620 W and 598 W to 493 W and 450 W for both 1 and 4 % SiO_2-water from 1 LPM to 5 LPM at 60 °C. It seems the increasing in the inlet temperature caused to

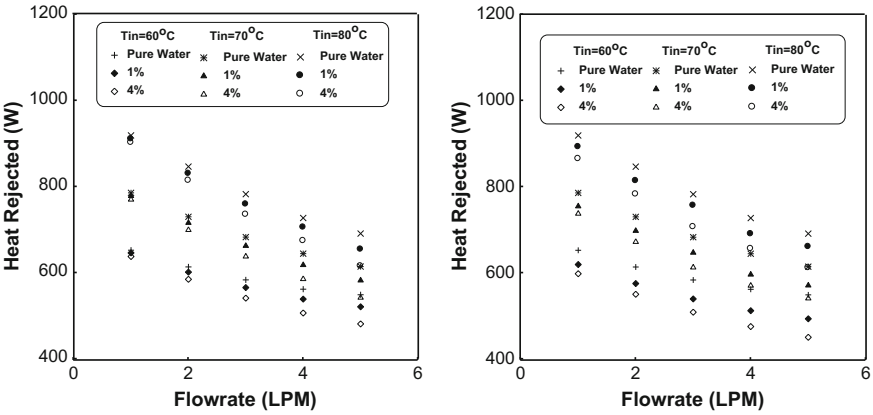

(a) TiO_2-Water (b) SiO_2-Water

Fig. 17 Heat rejected at different flowrate for the nanoparticles suspended to water

decrease in the heat rejected by 31 %. However, the increase in the volume fraction is due to decrease in the heat rejected by 3 %.

Figure 18a illustrates the heat rejected decreases from 647 W and 35 W to 571 W and 522 W for both 1 and 4 % TiO_2-EG from 3 LPM to 12 LPM at 60 °C. It seems the increasing in the inlet temperature caused to decrease in the heat rejected by 31 %. However, the increase in the volume fraction is due to decrease in the heat rejected by 3 %. Figure 18b shows the heat rejected decreases from 612 W and 598 W to 518 W and 465 w for both 1 and 4 % SiO_2-EG from 3 LPM to 12 LPM at 60 °C. It seems the increasing in the inlet temperature due to decrease in the heat rejected by 32 %. However, the increase in the volume fraction is due to decrease in the heat rejected by 4 %. Figure 19a indicates the heat rejected decreases from 556 W and 534 W to 333 W and 249 w for both 1 and 4 % TiO_2 suspended to 10 %EG + 90 %W from 3 LPM to 12 LPM at 60 °C. It seems the increasing in the inlet temperature caused to decrease in the heat rejected by 32.5 %. However, the increase in the volume fraction is due to decrease in the heat rejected by 4 %.

Figure 19b indicates the heat rejected decreases from 538 W and 508 W to 300 W and 209 w for both 1 and 4 % SiO_2 suspended to 10 %EG + 90 %W from 3 LPM to 12 LPM at 60 °C. It seems the increasing in the inlet temperature caused to decrease in the heat rejected by 33.5 %. However, the increase in the volume fraction is due to decrease in the heat rejected by 5 %.

Figure 20a indicates the heat rejected decreases from 556 W and 532 W to 334 W and 244 w for both 1 and 4 % TiO_2 dispersed to 20 %EG + 80 %W from 3 LPM to 12 LPM at 60 °C. It appears the increasing in the inlet temperature caused

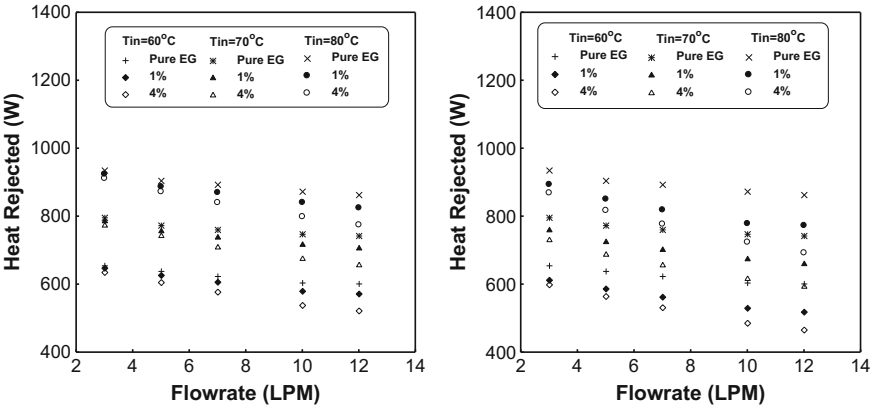

(a) TiO_2-EG (b) SiO_2-EG

Fig. 18 Heat rejected at different flowrate for the nanoparticles suspended to EG

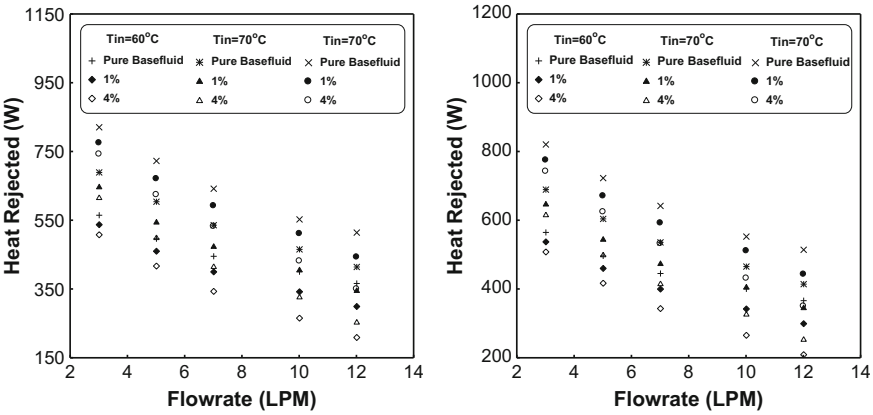

(a) TiO_2-10%EG+90%W (b) SiO_2-10%EG+90%W

Fig. 19 Heat rejected at different flowrate for the nanoparticles suspended to 10 %EG + 90 %W

to decrease in the heat rejected by 35 %. However, the increase in the volume fraction is due to decrease in the heat rejected by 5 %. Figure 20b indicates the heat rejected decreases from 537 and 509 W to 297 and 220 W for both 1 and 4 % SiO_2 dispersed to 20 %EG + 80 %W from 3 LPM to 12 LPM at 60 °C. It appears the increasing in the inlet temperature caused to decrease in the heat rejected by 33 %. However, the increase in the volume fraction is due to decrease in the heat rejected by 4 %.

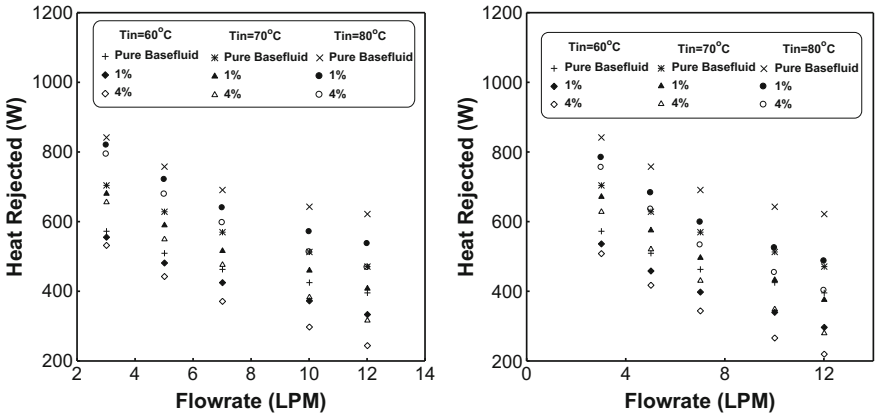

Fig. 20 Heat rejected at different flowrate for the nanoparticles suspended to 20 %EG + 80 %W

4.4 Heat Transfer Enhancement

The percentage of heat transfer enhancement depending on nanofluid volume concentration and inlet temperature to the radiator has been calculated by Eq (4.10). Figures 21 and 22 show the heat transfer enhancement depending on the nanofluid volume fraction and the inlet temperature, respectively.

It seems that the heat transfer enhancement increases with increasing of nanofluid volume concentration and inlet temperature, respectively. The values of heat transfer enhancement are from 12 to 31 % for TiO_2 nanofluid volume concentration from 1 to 4 % while the values of heat transfer enhancement are from 18 to 42 % for SiO_2 nanofluid volume concentration from 1 to 4 %. Likewise, the values of heat transfer enhancement are from 8 to 20 % for TiO_2 nanofluid at the inlet temperature from 60 to 80 °C, whereas the values of heat transfer enhancement are from 12 to 22 % for TiO_2 nanofluid at the inlet temperature from 60 °C to 80 °C. This refers to the nanofluid volume concentration affected more than the inlet temperature on the heat transfer enhancement, but significantly of using all of them. It can be seen the comparison of Nusselt number among nanofluids and base fluids at laminar flow. It appears that the nanofluid has higher values of the heat transfer enhancement than base fluid. It seems that the heat transfer enhancement for SiO_2 nanofluid is better than TiO_2 nanofluid by 80 %. In addition, the base fluid (20 % EG + 80 %W) has given higher values of the heat transfer than water by 60 %. On the other hand, the nanoparticles suspended to the base fluid (20 %EG + 80 %W) is the best type of the nanofluids due to the highest values of the heat transfer enhancement followed by 10 %EG + 90 %W then EG and finally water.

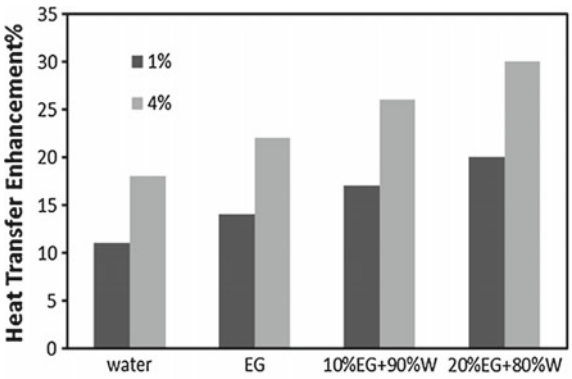

(a) TiO_2 nanofluid

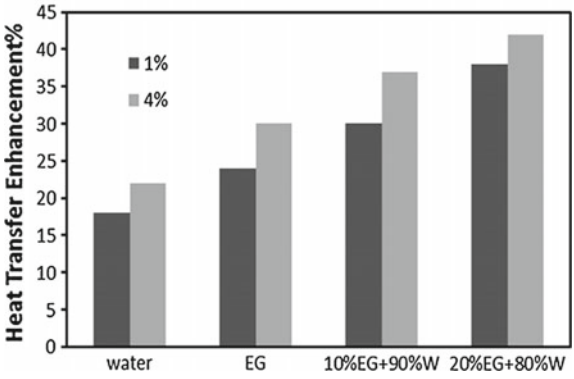

(b) SiO_2 nanofluid

Fig. 21 Effect of nanofluid volume fraction on the heat transfer enhancement

5 Conclusions and Recommendations

This chapter focuses on the conclusions derived from the results of the experiment and recommends further procedure and experiments which could have been done if limitations in experimental instruments and time were not a factor to conduct this research. In addition, CFD simulations have been successfully applied to solve the steady, laminar flow of a Newtonian fluid in the automotive cooling system. The results of this study have led to draw the following conclusions.

1. The density and specific heat capacity of the nanofluids and base fluids are studied. It seems significant increasing of the density with the increasing of volume fraction and decreasing of the temperature. On the other hand, there are significant decreasing of the specific heat capacity with the increasing of volume fraction and decreasing of the temperature.
2. There is a significant enhancement of the thermal conductivity measurement data with increase of both the volume fraction and the temperature.

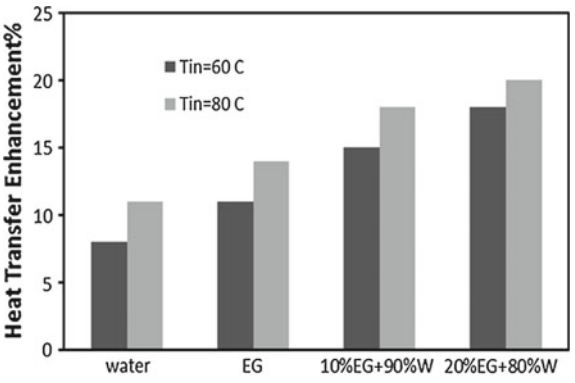

(a) TiO_2 nanofluid

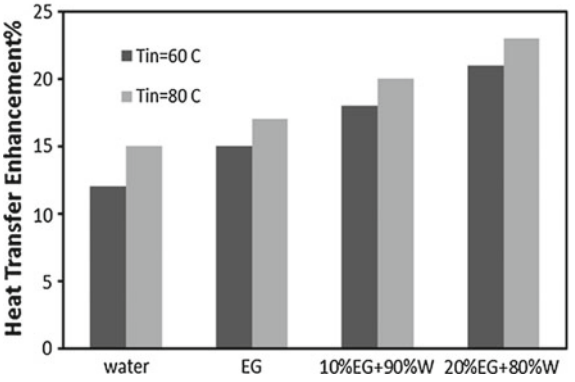

(b) SiO_2 nanofluid

Fig. 22 Effect of the inlet temperature on the heat transfer enhancement

3. The viscosity data measured decrease with the increasing of both the volume fraction and the temperature.
4. The friction factor decreases with the increase of Reynolds number and increases with the increase of the inlet temperature.
5. The heat transfer coefficient increases with the increase of both the volume fraction and the inlet temperature.
6. The outlet temperature increases with the increasing of the volume flowrate and the inlet temperature but decreases with the increase of the volume fraction.
7. The coolant heat transfer inside the flat tube increases with the increasing of the volume flowrate, the volume fraction, and the inlet temperature.
8. The heat rejected outside the cooling system decreases with the increasing of the volume flowrate and the volume fraction but increases with the increase of the inlet temperature.
9. Empirical correlations of the friction factor as a function of Reynolds number, Prandtl number, and the volume fraction for the nanofluids under the laminar

flow have been developed based on the experimental data. The deviations between correlations and the experimental data are not more than 3 %.

10. Empirical correlations of the Nusselt number as a function of Reynolds number, Prandtl number, and the volume fraction for the nanofluids under the laminar flow have been developed based on the experimental data. The deviations between correlations and the experimental data are not more than 6 %.
11. The aim of this thesis has been met to fabricate and build equipment that could be used to the nanoparticles suspended to base fluid replacement heat transfer water for automotive cooling system.

References

Abbasian, A. A., & Amani, J. (2012). Experimental study on the effect of TiO_2/water nanofluid on heat transfer and pressure drop. *Experimental Thermal and Fluid Science, 44*, 520–533.

Abdelrahman, M., Fumeaux, P., & Suter, P. (1979). Study of solid-gas-suspensions used for direct absorption of concentrated solar radiation. *Solar Energy, 22*(1), 45–48.

Ahuja, A. S. (1975). Augmentation of heat transport in laminar flow of polystyrene suspensions. *Journal of Applied Physics, 46*(8), 3408–3416.

Akoh, H., Tsukasaki, Y., Yaysuya, S., & Tasaki, A. (1978). Magnetic properties of ferromagnetic ultrafine particles prepared by vacuum evaporation on running oil substrate. *Journal of Crystal Growth, 45*, 495–500.

Andrew, L. T. (2008). Cooling system analysis, University of New South Wales at the Australian Defence Force Academy, Final Thesis Report.

ASHRAE. (2005). ASHRAE handbook: Fundamentals. *American Society of Heating, Refrigerating, and Air Conditioning Engineers*.

Bejan, A. (2004). *Convection heat transfer*. New York: John Wiley and Sons Inc.

Bozorgan, N., Krishnakumar, K., & Bozorgan, N. (2012). Numerical study on application of CuO-water nanofluid in automotive diesel engine radiator. *Modern Mechanical Engineering., 2*, 130–136.

Buongiorno, J. (2006). Convective transport in nanofluids. *Journal of Heat Transfer, 128*, 240–250.

Das, S. K., Choi, S. U. S., & Yu, W. (2007). *Nanofluids Science and Technology*. John Wiley and Sons, Inc.